

# Molecular characterization of G-protein-coupled receptor (GPCR) and protein kinase A (PKA) cDNA in *Perinereis aibuhitensis* and expression during benzo(a)pyrene exposure

Huang Yi<sup>Equal first author, 1</sup>, Sun Jia<sup>Equal first author, 1</sup>, Han Ping<sup>1</sup>, Zhao Heling<sup>2</sup>, Wang Mengting<sup>1</sup>, Zhou Yibing<sup>1</sup>, Yang Dazuo<sup>1</sup>, Zhao Huan<sup>Corresp. 1</sup>

<sup>1</sup> College of Fisheries And Life Science, Dalian Ocean University, Dalian, Liaoning, China

<sup>2</sup> Asian Herpetological Research Editorial Office, Chengdu Institute of Biology, Chinese Academy of Sciences, Cheng du, Sichuan, China

Corresponding Author: Zhao Huan  
Email address: zhaohuan@dloou.edu.cn

**Background.** G-protein-coupled receptors (GPCRs) are one of the most important molecules that transfer signals across the plasma membrane, and play central roles in physiological systems. The molecular architecture of GPCRs allows them to bind to diverse chemicals, including environmental contaminants.

**Methods.** To investigate the effects of benzo(a)pyrene (B[a]p) on GPCR signaling, GPCR and the protein kinase A (PKA) catalytic subunit of *Perinereis aibuhitensis* were cloned. The expression patterns of these two genes during B(a)p exposure were determined with real-time fluorescence quantitative PCR.

**Results.** The full-length cDNAs of PaGPCR and the PaPKA catalytic subunit were 1,514 and 2,662 nucleotides, respectively, encoding 339 and 351 amino acids, respectively. Multiple sequence alignments indicated that the deduced amino acid sequence of PaGPCR shared a low level of similarity with the orphan GPCRs of polychaetes and echinoderms, whereas PaPKA shared a high level of identify with the PKA catalytic subunits of other invertebrates. B(a)p exposure time-dependently elevated the expression of PaGPCR and PaPKA. The expression of both PaGPCR and PaPKA was also dose-dependent, except at a dose of 10 µg/L B(a)p.

**Discussion.** These results suggested that GPCR signaling in *P. aibuhitensis* was involved in the polychaete's response to environmental contaminants.

1 **Molecular characterization of G-protein-coupled receptor**  
2 **(GPCR) and protein kinase A (PKA) cDNA in *Perinereis***  
3 ***aibuhitensis* and expression during benzo(a)pyrene exposure**

4 Huang Yi<sup>1</sup>, Sun Jia<sup>1</sup>, Han Ping<sup>1</sup>, Zhao Heling<sup>2</sup>, Wang Mengting<sup>1</sup>, Zhou Yibing<sup>1</sup>, Yang Dazuo<sup>1</sup>

5 <sup>1</sup>Key Laboratory of Marine Bio-Resources Restoration and Habitat Reparation in Liaoning Province,  
6 Dalian Ocean University, Dalian, Liaoning, China

7 <sup>2</sup>Asian Herpetological Research Editorial Office, Chengdu Institute of Biology, Chinese Academy of  
8 Sciences, Chengdu, Sichuan, China

9

10 Corresponding Author:

11 Zhao Huan<sup>1</sup>

12 Shahekou District Heishijiao street No.52, Dalian, Liao ning, 116023, China

13 Email address: zhaohuan@dlou.edu.cn;15206936767@163.com

14

15

16

17

18

19

20

21

22

23

24

25

26

27

28

29

30

31

32

33

## 34 Abstract

35 **Background.** G-protein-coupled receptors (GPCRs) are one of the most important molecules  
36 that transfer signals across the plasma membrane, and play central roles in physiological  
37 systems. The molecular architecture of GPCRs allows them to bind to diverse chemicals,  
38 including environmental contaminants.

39 **Methods.** To investigate the effects of benzo(a)pyrene (B[a]p) on GPCR signaling, GPCR and  
40 the protein kinase A (PKA) catalytic subunit of *Perinereis aibuhitensis* were cloned. The  
41 expression patterns of these two genes during B(a)p exposure were determined with real-time  
42 fluorescence quantitative PCR.

43 **Results.** The full-length cDNAs of PaGPCR and the PaPKA catalytic subunit were 1,514 and  
44 2,662 nucleotides, respectively, encoding 339 and 351 amino acids, respectively. Multiple  
45 sequence alignments indicated that the deduced amino acid sequence of PaGPCR shared a low  
46 level of similarity with the orphan GPCRs of polychaetes and echinoderms, whereas PaPKA  
47 shared a high level of identify with the PKA catalytic subunits of other invertebrates. B(a)p  
48 exposure time-dependently elevated the expression of *PaGPCR* and *PaPKA*. The expression of  
49 both *PaGPCR* and *PaPKA* was also dose-dependent, except at a dose of 10 µg/L B(a)p.

50 **Discussion.** These results suggested that GPCR signaling in *P. aibuhitensis* was involved in the  
51 polychaete's response to environmental contaminants.

## 52 Introduction

53 Benzo(a)pyrene (B(a)P), a kind of polycyclic aromatic hydrocarbon (PAH), can cause genetic  
54 damage, immune and endocrine dysfunction, and malformation in humans and other organisms.  
55 Its high lipophilicity allows it to absorb to organic matter and other particulate matter and thus  
56 accumulate in sediments. Recent increases in offshore oil production and transportation and the  
57 sewerage discharge of domestic and industrial wastewater have led to environmental pollution in  
58 coastal regions, and B(a)P has been widely detected in sediments around the world, even in  
59 China. The levels of B(a)P in the sediments of Dalian Bay vary from 10.5 to 3421.2 ng/g (Zhang,

60 2008), and in the sediments around the drilling platform in the Bohai Sea, the concentration of  
61 B(a)p is up to 27.69 ng/g (Yang et al, 2016). PAHs such as B(a)p can be absorbed by benthic  
62 organisms via ingestion and through their body surfaces, and B(a)p is reported to have serious  
63 effects on deposit feeders. Therefore, the toxicity and bioavailability of B(a)p are important  
64 factors in the assessment of sediment pollution.

65 G-protein-coupled receptors (GPCRs) are the largest superfamily of cell membrane proteins  
66 (Fredriksson et al, 2003). The molecular architecture of the GPCRs allows them to bind to  
67 diverse organic and inorganic molecules. GPCRs mediate cell proliferation and survival by  
68 transmitting signals from a range of extracellular ligands across the cell membrane to signaling  
69 pathways. In vertebrates, they are key regulators of the innate and adaptive immune responses  
70 and have been investigated as potential targets in drug discovery (Garland, 2013). However,  
71 examples of GPCRs in invertebrates are limited. Miller et al. (2015) reported that  
72 *Caenorhabditis elegans* with mutations in the GPCR follicle-stimulating hormone receptor 1  
73 (FSHR-1) died significantly more quickly in the presence of cadmium than wild-type nematodes,  
74 which suggests that this GPCR pathway protects the nematode against cadmium-induced  
75 damage. They also found that FSHR-1 antagonizes the capacity of *C. elegans* to resist cold  
76 stress, and the mutants lacking *fshr-1* survived better than wild-type worms at low temperatures.  
77 Dong and Zhang (2012) identified a putative GPCR gene, *HP1R*, in the red swamp crayfish  
78 *Procambarus clarkia*, and the expression of *HP1R* was significantly increased in the presence of  
79 Gram-negative bacteria.

80 Because of the aromatic structures present a number of GPCR ligands, GPCRs are potential  
81 targets of aromatic pollutants such as B(a)p (Ferrec and Ovrevik, 2018). Mayati et al. (2012)  
82 reported the interaction between B(a)p and the  $\beta_2$ -adrenergic receptor ( $\beta_2$ ADR) in endothelial  
83 HMEC-1 cells and the consequent increase in intracellular  $Ca^{2+}$ , which influenced the expression  
84 of cytochrome P450 B1. This suggests that  $\beta_2$ ADR, a kind of GPCR, is potentially involved in  
85 the deleterious effects of PAHs. Factor et al. (2011) also observed the reduced expression and  
86 function of  $\beta_2$ ADR in airway epithelial cells and smooth muscle cells after their exposure to a  
87 mixture of PAHs. This implies that the  $\beta_2$ ADR signal transduction pathway is affected by PAHs.  
88 These data indicate that PAHs, including B(a)p, modulate the concentrations of intracytosolic  
89 cyclic adenosine monophosphate (cAMP) or  $Ca^{2+}$  via G-protein-dependent mechanisms (Bainy,  
90 2007; Nadal et al., 2000).

91 The marine polychaete *Perinereis aibuhitensis* is widely distributed in the mudflats and  
92 estuarine sediments that occur widely along the coasts of Southeast Asia. They spend most of  
93 their lives within the sediments, ensuring their continuous contact with any sediment-associated  
94 contaminants. Chen et al. (2012) identified a *CYP4* gene of *P. aibuhitensis* and showed that  
95 exposure to petroleum hydrocarbons significantly induce the expression of this gene. To clarify  
96 whether GPCRs were involved in modulating the toxicity of aromatic pollutants, the full-length  
97 GPCR and protein kinase A (PKA) cDNAs were cloned and the expression patterns of these two  
98 genes were determined in this study. Our results provide important information on the function  
99 of GPCRs in polychaetes.

## 100 **Materials & Methods**

### 101 **B(a)p exposure**

102 *Perinereis aibuhitensis* specimens (10–15 cm,  $2.0 \pm 0.5$  g wet weight) were collected from an  
103 estuary of Jinzhou Bay in Dalian, China. The animals were transferred to the laboratory and  
104 acclimatized in filtered seawater (salinity 31–32, temperature  $16 \pm 0.5^\circ\text{C}$ ) for a week before the  
105 experiment. During acclimatization, the *P. aibuhitensis* were fed a powdered mix containing kelp  
106 powder, gulfweed powder, fishmeal, yeast, and spirulina. The worms were deprived of food  
107 during their exposure to B(a)P.

108 Based on the standard seawater quality of the People's Republic of China (GB 3097-1997),  
109 four B(a)P concentration groups were established: 0.5, 5, 10, and 50  $\mu\text{g/L}$ . A blank control  
110 (seawater only) group and an acetone solvent group (100  $\mu\text{L/L}$ ) were also established. Three  
111 repetitions of each concentration group were set up. Ten worms were randomly placed in 2L  
112 beakers containing different concentrations of B(a)P. During the experiment, the temperature of  
113 the seawater was  $16 \pm 0.5^\circ\text{C}$ , and the seawater was renewed every 24h. On days 4, 7, and 14 of  
114 the experiment, four individuals were randomly sampled from each concentration group, and the  
115 body wall was removed and preserved at  $-80^\circ\text{C}$ .

### 116 **Cloning the full-length GPCR and PKA cDNAs of *P. aibuhitensis***

117 Each sample was ground to powder and the total RNA was extracted with RNAiso™ Plus  
118 (TaKaRa, Dalian, China). The quality of the RNA was determined with 1% agarose gel  
119 electrophoresis. The RNA (500 ng) was reverse transcribed to cDNA for the rapid amplification  
120 of cDNA ends (RACE) using the SMARTer® RACE Kit (Clontech, Palo Alto, CA, USA). The  
121 3' and 5' RACE primers were designed with the Primer 5.0 software (PREMIER Biosoft, Palo  
122 Alto, CA, USA) according to the confirmed partial sequences of GPCR and PKA obtained from  
123 *P. aibuhitensis* transcriptome sequences. The primers used in this study are shown in Table 1.

124 The 3' RACE amplification of *P. aibuhitensis* GPCR (*PaGPCR*) was performed using the 3'  
125 RACE cDNA as the template. The PCR system (50  $\mu\text{L}$ ) for *PaGPCR* contained 15.5  $\mu\text{L}$  of PCR-  
126 grade water, 25.0  $\mu\text{L}$  of 2× SeqAmp Buffer, 1.0  $\mu\text{L}$  of SeqAmp DNA Polymerase, 2.5  $\mu\text{L}$  of 3'  
127 RACE cDNA, 5.0  $\mu\text{L}$  10 × UPM (Universal Primer Mixture), and 1.0  $\mu\text{L}$  of primer GPCR-F1  
128 (10  $\mu\text{M}$ ). The thermal cycling conditions were: 35 cycles of denaturation at  $94^\circ\text{C}$  for 30 s,  
129 annealing at  $65^\circ\text{C}$  for 30s, and extension at  $72^\circ\text{C}$  for 3 min. The 3' RACE amplification of  
130 *PaPKA* was performed with nested PCR. The outer PCR reaction system for *P. aibuhitensis* PKA  
131 (*PaPKA*) was the same as that for *PaGPCR*, except that a specific primer was used. The reaction  
132 conditions for the outer PCR were: 35 cycles of denaturation at  $94^\circ\text{C}$  for 30 s, annealing at  
133  $63.9^\circ\text{C}$  for 30 s, and extension at  $72^\circ\text{C}$  for 3 min. The outer PCR product (5.0  $\mu\text{L}$ ) was diluted  
134 with 245  $\mu\text{L}$  of TE buffer, and 5.0  $\mu\text{L}$  of the diluted product was used as the template for the  
135 inner PCR. The reaction conditions and system for the inner PCR were the same as for the outer  
136 PCR of *PaPKA*.

137 The 5' RACE product of *PaGPCR* was amplified with nested PCR. The outer PCR reaction  
138 system (50  $\mu\text{L}$ ) for *PaGPCR* contained 15.5  $\mu\text{L}$  of PCR-grade water, 25.0  $\mu\text{L}$  of 2× SeqAmp

139 Buffer, 1.0  $\mu\text{L}$  of SeqAmp DNA Polymerase, 2.5  $\mu\text{L}$  of 5' RACE DNA, 5.0  $\mu\text{L}$  of  $10 \times$  UPM,  
140 and 1.0  $\mu\text{L}$  of primer GPCR-R1 (10  $\mu\text{M}$ ). The reaction conditions for the outer PCR were: 35  
141 cycles of denaturation at  $94^\circ\text{C}$  for 30 s, annealing at  $60^\circ\text{C}$  for 30 s, and extension at  $72^\circ\text{C}$  for 3  
142 min. The outer PCR product (5.0  $\mu\text{L}$ ) of *PaGPCR* was diluted with 245  $\mu\text{L}$  of TE buffer and 5.0  
143  $\mu\text{L}$  of the diluted product was used as the template for the inner PCR. The reaction system (50  
144  $\mu\text{L}$ ) for the inner PCR of *PaGPCR* contained 5.0  $\mu\text{L}$  of the diluted outer PCR product, 17.0  $\mu\text{L}$  of  
145 PCR-grade water, 25.0  $\mu\text{L}$  of  $2 \times$  SeqAmp Buffer, 1.0  $\mu\text{L}$  of SeqAmp DNA Polymerase, 1.0  $\mu\text{L}$   
146 of UPM Short, and 1.0  $\mu\text{L}$  of primer GPCR-R2 (10  $\mu\text{M}$ ). The reaction conditions were: 20 cycles  
147 of denaturation at  $94^\circ\text{C}$  for 30 s, annealing at  $60^\circ\text{C}$  for 30 s, and extension at  $72^\circ\text{C}$  for 3 min. The  
148 5' RACE product of PaPKA was amplified with ordinary PCR, and the reaction system and  
149 conditions were the same as those for PaGPCR.

150 The PCR products were detected with 1% agarose gel electrophoresis and purified with the  
151 Agarose Gel DNA Purification Kit (Tiangen, Beijing, China), according to the manufacturer's  
152 instructions. The PCR products were sequenced by TaKaRa Biotechnology Co. Ltd.

### 153 **Bioinformatic analysis of PaGPCR and PaPKA**

154 The amino acid sequences of PaGPCR and PaPKA were deduced with the Expert Protein  
155 Analysis System (<http://www.us.expasy.org/tools>). The conserved domain in each amino acid  
156 sequence was analyzed with the Motif Scan (<http://www.hits.isbsib.ch/cgi-bin/PESCAN>) and  
157 Expasy (<http://www.au.expasy.org/prosite/>). The protein localization sites in the cell were  
158 predicted with the Psort software (<http://psort.hgc.jp/form2.html>). The transmembrane (TM)  
159 helices in the protein were predicted with the TMHMM software  
160 (<http://www.cbs.dtu.dk/services/TMHMM/>). The tertiary structures of GPCR and PKA were  
161 predicted with the Swiss-Model software (<http://swissmodel.expasy.org/interactive>). Multiple  
162 sequences were aligned with the Clustal W software (<http://www.ebi.ac.uk/clustalW>).  
163 Phylogenetic analyses of GPCR and PKA were performed in MEGA 5.0. The tree topologies  
164 were evaluated with bootstrapping, using 1,000 replicates.

### 165 **Expression of PaGPCR and PaPKA genes during B(a)p exposure**

166 Real-time fluorescence quantitative PCR was used to investigate the expression of the two genes  
167 in *P. aibuhitensis* during B(a)p exposure. The  $\beta$ -actin gene was used as the reference gene,  
168 according to our previous study (*Li et al., 2018*). The primer information is shown in Table 1.  
169 Amplification was performed in 20  $\mu\text{L}$  reactions containing 10  $\mu\text{L}$  of SYBR Premix Ex Taq II  
170 (Tli RNaseH Plus) (TaKaRa, Dalian, China), 0.8  $\mu\text{L}$  of each primer (10  $\mu\text{M}$ ), 0.4  $\mu\text{L}$  of  $50 \times$  ROX  
171 Reference Dye II, 2.0  $\mu\text{L}$  of cDNA, and 6.0  $\mu\text{L}$  of  $\text{H}_2\text{O}$ . The reaction conditions were:  $95^\circ\text{C}$  for  
172 30 s, then 40 cycles of  $95^\circ\text{C}$  for 5 s and  $60^\circ\text{C}$  for 34 s. The melting curves were analyzed after  
173 the real-time quantitative analyses. The standard curves were tested with serial 10-fold sample  
174 dilutions. The slopes of the standard curves and the PCR efficiency were calculated to confirm  
175 the accuracy of the real-time PCR data.

### 176 **Statistical analysis**

177 The relative quantitative ( $2^{-\Delta\Delta\text{Ct}}$ ) method was used to analyze the expression of the *GPCR* and  
178 *PKA* genes. The data are expressed as means  $\pm$  standard deviations (SD), and one-way analysis

179 of variance was used to analyze the significance of the differences among the different  
180 concentration groups at each sampling point, with the SPSS 19.0 software.  $P$  values  $\leq 0.05$  were  
181 considered statistically significant.

## 182 Results

### 183 Molecular characterization of *PaGPCR*

184 The full-length cDNA of *PaGPCR* was 1,514 bp and included a 5' untranslated region (UTR) of  
185 213 bp, a 3' UTR of 284 bp, and an open reading frame (ORF) of 1,017 bp, encoding 338 amino  
186 acids with a predicted molecular weight of 38.799 kDa and a theoretical isoelectric point of 9.38  
187 (Figure 1). This nucleotide sequence was deposited in the GenBank database under accession  
188 number KX792261. The seven-transmembrane (7TM)-helix bundle (304–1,146 bp) that defines  
189 the GPCR protein family was present in *PaGPCR*. The glutamic acid/aspartic acid-arginine-  
190 tyrosine (E/DRY) motif (amino acids 124–126) at the border between TM III and intracellular  
191 loop 2 and the NPXXY motif (amino acids 298–302) of TM VII near the inner cell membrane  
192 were detected in the deduced protein sequence, indicating that the protein sequence belonged to  
193 the rhodopsin family. In an amino acid comparison, *PaGPCR* shared 33% similarity with the  
194 orphan GPCR of *Platynereis dumerilii* and 30%–33% similarity with galanin receptor type 2 of  
195 echinoderms (Figure 2).

196 The predicted cellular localization of the *PaGPCR* protein showed it mostly located on the cell  
197 membrane (52.2%), and seven TM helices were predicted in the deduced protein sequence  
198 (Figure 3). The three-dimensional structural analysis of *PaGPCR* showed that it contained seven  
199  $\alpha$ -helices, similar to the GPCRs of other animals (Figure 4). Its three-dimensional structure and  
200 protein localization confirmed that this protein sequence was a GPCR.

### 201 Molecular characterization of *PaPKA*

202 The total length of *P. aibuhitensis* PKA cDNA was 2662 bp, containing a 3' UTR of 1,483 bp, a  
203 5' UTR of 126 bp, and an ORF of 1,053 bp encoding 350 amino acids (Figure 5). The predicted  
204 molecular weight of *PaPKA* was 40.28 kDa and its theoretical isoelectric point was 8.35. The  
205 nucleotide sequence was deposited in GenBank under accession number KX839259. A glycine-  
206 rich loop GTGSFGRV (amino acids 50–57), Ser/Thr active site RDLKPEN (amino acids 165–  
207 171), PKA-regulatory-subunit-binding site LCGTPEY (amino acids 198–204), DFG triplet  
208 (Asp–Phe–Gly) for orienting the  $\gamma$ -phosphates of adenosine triphosphate (ATP) for transfer, APE  
209 motif (Ala–Pro–Glu) to stabilize the structure of the large lobe of PKA, and conserved  
210 phosphorylation site (Thr197) were detected in this deduced amino acid sequence. The presence  
211 of these conserved regions indicated that *PaPKA* was the catalytic subunit of PKA. An amino  
212 acid comparison indicated that *PaPKA* was highly similar to other PKA catalytic subunits  
213 (Figure 6).

214 The predicted location of *PaPKA* in the cell was predominantly in the cytoplasm (47.8%). The  
215 three-dimensional structural analysis of *PaPKA* showed that it folded into a two-lobed structure  
216 (Figure 7). The small lobe had a predominantly  $\beta$ -sheet structure, which was responsible for  
217 anchoring and orienting the nucleotide, and the large lobe had a predominantly  $\alpha$ -helix structure,

218 and was primarily involved in binding the peptide substrate and initiating phosphotransfer  
219 (*Hanks and Hunter, 1995*). Ser53, Phe54, and Gly55 formed hydrogen bonds with ATP  $\beta$ -  
220 phosphate oxygens, and Leu49 and Val57 formed a hydrophobic pocket enclosing the adenine  
221 ring of ATP.

### 222 **Phylogenetic analysis of PaGPCR and PaPKA**

223 Phylogenetic trees were constructed from the amino acid sequences of GPCR and PKA, (Figure  
224 8 and Figure 9, respectively). Figure 8 indicates that PaGPCR shared great identity with the  
225 orphan GPCRs of other polychaetes. Figure 9 shows that PaPKA shared identity with mollusk  
226 PKAs, which clustered together on a single branch.

### 227 **Effects of B(a)P on PaGPCR and PaPKA expression in *P. aibuhitensis***

228 Figure 10A shows the expression of the *PaGPCR* gene of *P. aibuhitensis* during B(a)p exposure.  
229 There was no difference in its expression between the acetone control group and the blank  
230 control group, indicating that acetone as a solvent had no toxic effect on the nematodes. During  
231 exposure to B(a)p, the expression of the *PaGPCR* gene increased both time- and approximately  
232 dose-dependently. On day 4, *PaGPCR* expression was significantly upregulated ( $P < 0.05$ ) in all  
233 but the 0.5  $\mu\text{g/L}$  B(a)P group. The expression of *PaGPCR* in the 5, 10, and 50  $\mu\text{g/L}$  B(a)P groups  
234 was 2.32-, 3.46-, and 3.15-fold higher than in the control group, respectively. On day 7, the  
235 expression of *PaGPCR* in the 0.5, 5, 10, and 50  $\mu\text{g/L}$  B(a)P groups was 3.10-, 2.91-, 3.59-, and  
236 3.28-fold higher than in the control group, respectively ( $P < 0.05$ ). The expression of *PaGPCR* in  
237 each concentration group reached its highest level on day 14, at 4.30-, 6.60-, 4.79-, and 6.36-fold  
238 higher than the control group, respectively ( $P < 0.01$ ).

239 The expression pattern of the *PaPKA* gene during B(a)P exposure was the same as that of  
240 *PaGPCR* (Figure 10B). The expression of *PaPKA* increased as the time of exposure increased.  
241 On day 4, the expression of *PaPKA* was slightly higher in all but the 0.5  $\mu\text{g/L}$  B(a)p  
242 concentration group, at 1.79-, 1.21-, and 2.21-fold higher in the 5, 10, and 50  $\mu\text{g/L}$  B(a)P groups,  
243 respectively, than in the control group. The expression of *PaPKA* in each concentration group  
244 was higher on day 7 than on day 4, at 1.25-, 1.90-, 2.52-, and 2.89-fold higher in the 0.5, 5, 10,  
245 and 50  $\mu\text{g/L}$  B(a)P groups, respectively, than in the control group ( $P < 0.05$ ). On day 14, the  
246 expression of *PaPKA* reached its highest level in each concentration group, at 3.19-, 5.03-, 3.10-,  
247 and 5.02-fold higher than the control group, respectively ( $P < 0.05$ ).

## 248 **Discussion**

249 To investigate the reaction of GPCR to B(a)p exposure in *P. aibuhitensis*, the full-length cDNAs  
250 of the *PaGPCR* and *PaPKA* were isolated and characterized in *P. aibuhitensis* for the first time.  
251 The sequence of *PaGPCR* contained 1514 bp, encoding 338 amino acids. The deduced protein  
252 sequence of PaGPCR contained a 7TM helix bundle domain, flanked by the extracellular N-  
253 terminal region and the intracellular C-terminus. As part of the functional mechanism of GPCR,  
254 the E/DRY motif (amino acids 124–126), which plays an important role in regulating the  
255 conformational state of GPCR, occurred at the border between TM III and intracellular loop 2 in  
256 this sequence. The protein sequence of PaGPCR also contained the NPXXY motif (amino acids  
257 298–302) in TM VII, which confirmed that it belonged to the rhodopsin family, the largest of the

258 five families involved in many signaling processes (*Fredriksson et al., 2003*). A multiple protein  
259 sequence alignment showed that PaGPCR shared almost 33% homology with the galanin  
260 receptor of echinoderms. A phylogenetic analysis showed that it clustered most closely with the  
261 orphan GPCRs of other polychaetes, and the galanin receptor of echinoderms. It is well-known  
262 that proteins with similar sequences often display comparable functions if the sequence identity  
263 exceeds 30% (*Kakarala and Jamil, 2014*). However, a prediction based on sequence identity  
264 alone may not be reliable. Therefore, further study is needed to prove the function of PaGPCR.  
265 In contrast to the low sequence identity of GPCR, PKA in *P. aibuhitensis* shared high sequence  
266 identity with the PKA catalytic subunits of other species. *PaPKA* contained 2,662 bp, which  
267 encoded 350 amino acids. The deduced amino acid sequence of PaPKA contained all the  
268 conserved domains that were necessary for kinase activity, such as the conserved Thr in the  
269 activation loop, the ATP-binding site (GTGSFGRV), the serine/threonine kinase active site  
270 (RDLKPEN), and the PKA-regulatory-subunit-binding site (LCGTPEY). The highly conserved  
271 amino acids at the ATP-binding site played important roles in ATP binding and phosphotransfer.  
272 The high homology among the PKA catalytic subunits suggested that they have a conserved role  
273 in intracellular signaling in both vertebrates and invertebrates.

274 GPCRs comprise the largest and most important family of cell-surface proteins, transmitting  
275 signals from extracellular ligands. In vertebrates, they are key regulators of the innate and  
276 adaptive immune responses and have been used as potential targets in drug discovery (*Garland,*  
277 *2013*). However, they have been inadequately investigated in invertebrates. *Miller et al. (2015)*  
278 reported that FSHR-1 mutants of *C. elegans* died significantly more quickly during cadmium  
279 exposure than wild-type nematodes, which suggests that the GPCR pathway protects *C. elegans*  
280 against pollutant damage. *Dong and Zhang (2012)* reported that Gram-negative bacterial  
281 infection induced the expression of the *HP1R* gene in *Procambarus clarkia*. In the present study,  
282 we found that B(a)p exposure induced the expression of *PaGPCR*, which increased with time in  
283 each concentration group. This result was similar to reports in other invertebrates, and implied  
284 that GPCR played an important role in reducing the deleterious effects of B(a)p in *P.*  
285 *aibuhitensis*. GPCRs interact with diverse chemical structures, which increases cAMP  
286 production, which then stimulates phospholipase C activity and the subsequent mobilization of  
287  $Ca^{2+}$ . *Mayati et al. (2012)* observed an interaction between B(a)p and  $\beta_2$ ADR in endothelial  
288 HMEC-1 cells, which altered the levels of intracellular  $Ca^{2+}$  and the expression of cytochrome  
289 P450 B1. *Factor et al. (2011)* observed the reduced expression and function of  $\beta_2$ ADR in airway  
290 epithelial cells and smooth muscle cells after their exposure to a mixture of PAHs. In the present  
291 study, we also observed that the expression of *PaPKA* in *P. aibuhitensis*, was higher during  
292 B(a)p exposure than the control level in all but the 0.5  $\mu$ g/L B(a)p concentration group. The  
293 expression of *PaPKA* was significantly and exposure-time-dependently induced by 50  $\mu$ g/L  
294 B(a)p. The increased expression of *PaPKA* and *PaGPCR* suggested that the GPCR signal  
295 transduction pathway in *P. aibuhitensis* was affected by PAHs.

296 B(a)p can be metabolized by organisms through a series of enzymatic and nonenzymatic  
297 reactions. Typically, B(a)p is metabolized by the phase I enzyme cytochrome P450 (CYP) and

298 phase II enzymes such as glutathione S-transferase (GST). The induction of CYP gene  
299 expression has been detected in *P. aibuhitensis* (Chen et al., 2012; Zhao et al., 2014). In  
300 vertebrates, the induction of the CYP enzymes involved in the biotransformation of PAHs is  
301 mediated by the aryl hydrocarbon receptor (AhR) pathway. Both  $\alpha$ - and  $\beta$ -type AhR proteins  
302 have been reported in bivalves (Fabbri and Capuzzo, 2010). However, no AhR homologues have  
303 been identified in other invertebrates, including marine polychaetes (Jorgensen et al., 2008).  
304 Ferrec and Ovrevik (2018) reported that a number of GPCR ligands contain aromatic structures,  
305 and that B(a)p modulates the concentration of intracytosolic cAMP through the GPCR pathway  
306 without the involvement of conventional nuclear receptors. In this study, we demonstrated the  
307 induction of *GPCR* and *PKA* expression during B(a)p exposure, so we hypothesized that the  
308 GPCR pathway is also involved in the biotransformation of PAHs in *P. aibuhitensis*. Further  
309 study of the relationship between GPCR and CYP expression is required to test our hypothesis.

## 310 Conclusions

311 GPCR represents a critical point of contact between cells and their surrounding environments.  
312 This is the first study in which *P. aibuhitensis* GPCR and PKA cDNAs have been cloned. We  
313 have also demonstrated that the expression of *GPCR* and *PKA* was induced in *P. aibuhitensis* by  
314 B(a)p exposure, and that their expression was affected, to some extent, by the B(a)p  
315 concentration and the exposure time. These results should be useful in investigating the  
316 biotransformation of PAHs by marine polychaetes.

## 317 Acknowledgements

318 This work was funded by the National Natural Science Foundation of China (No. 41306138), the  
319 key laboratory of mariculture and stock enhancement in North China's Sea, Ministry of  
320 Agriculture and Rural Affairs, Dalian Ocean unversity, P. R. China(2018-KF-15) and Liaoning  
321 Scientific instrument sharing Platform(L201810).

## 322 References

- 323 **Bainy AC. 2007.** Nuclear receptors and susceptibility to chemical exposure in aquatic  
324 organisms. *Environment International* **33(4)**:571-575 DOI 10.1016/j.envint.2006.11.004
- 325 **Chen X, Zhou YB, Yang DZ, Zhao H, Wang LL, Yuan XT. 2012.** CYP4 mRNA expression in  
326 marine polychaete *Perinereis aibuhitensis* in response to petroleum hydrocarbon and  
327 deltamethrin. *Marine Pollution Bulletin* **64(9)**:1782-1788 DOI  
328 10.1016/j.marpolbul.2012.05.035
- 329 **Dong C, Zhang P. 2012.** A putative G protein-coupled receptor involved in innate immune  
330 defense of *Procambarus clarkii* against bacterial infection. *Comp Biochem Physiol A Mol*  
331 *Integr Physiol* **161(2)**:95-101 DOI 10.1016/j.cbpa.2011.09.006

- 332 **Fredriksson R, Malin CL, Lundin LG, Helgi BS. 2003.** The G-protein-coupled receptors in  
333 the human genome form five main families. *Molecular Pharmacology* **63(6)**:1256-1272 DOI  
334 10.1124/mol.63.6.1256
- 335 **Factor P, Akhmedov AT, McDonald JD, Qu A, Wu J, Jiang H, Dasgupta T, Panettieri Jr**  
336 **RA, Perera F, Miller RL. 2011.** Polycyclic aromatic hydrocarbons impair function of b2-  
337 adrenergic receptors in airway epithelial and smooth muscle cells. *American Journal of*  
338 *Respiratory Cell & Molecular Biology* **45(5)**:1045-1049 DOI 10.1165/rcmb.2010-0499OC
- 339 **Fabbri E, Capuzzo A. 2010.** Cyclic AMP signaling in bivalve molluscs: an overview. *Journal*  
340 *of Experimental Zoology Part A Ecological Genetics & Physiology* **313A(4)**:179-200 DOI  
341 10.1002/jez.592
- 342 **Ferrec E, Øvrevik J. 2018.** G-protein coupled receptors (GPCR) and environmental exposure.  
343 Consequences for cell metabolism using the  $\beta$ -adrenoceptors as example. *Current Opinion in*  
344 *Toxicology* **8**:14-19 DOI 10.1016/j.cotox.2017.11.012
- 345 **Garland SL. 2013.** Are GPCRs still a source of new targets? *Journal of Biomolecular Screening*  
346 **18**:947-966 DOI 10.1177/1087057113498418
- 347 **Hanks SK, Hunter T. 1995.** Protein kinases 6. The eukaryotic protein kinase superfamily:  
348 kinase (catalytic) domain structure and classification. *The FASEB Journal* **9(8)**:576-596 DOI  
349 10.1096/fasebj.9.8.7768349
- 350 **Jorgensen A, Giessing AMB, Rasmussen LJ, Andersen O. 2008.** Biotransformation of  
351 polycyclic aromatic hydrocarbons in marine polychaetes. *Marine environmental* **65 (2)**:171-  
352 186 DOI 10.1016/j.marenvres.2007.10.001
- 353 **Kakarala KK, Jamil K. 2014.** Sequence-structure based phylogeny of GPCR Class A  
354 Rhodopsin receptors. *Molecular Phylogenetics and Evolution* **2,74**:66-96 DOI  
355 10.1016/j.ympev.2014.01.022
- 356 **Li WJ, Xue SL, Pang Min, Yue ZH, Yang DZ, Zhou YB, Zhao H. 2018.** The expression  
357 characteristics of vitellogenin(VTG) in response to B(a)p exposure in polychaete *Perinereis*  
358 *aibuhitensis*. *Journal of Oceanology and Limnology* **36(06)**:399-409 DOI 10.1007/s00343-  
359 019-7304-0
- 360 **Miller RL, Thompson AA, Trapella C, Guerrini R, Malfacini D, Patel N, Han GW**  
361 **Cherezov V, Caló G, Katritch V, Stevens RC. 2015.** The importance of ligand-receptor  
362 conformational pairs in stabilization: spotlight on the N/OFQ G protein-coupled receptor.  
363 *Structure* **23(12)**: 2291-2299 DOI 10.1016/j.str.2015.07.024
- 364 **Mayati A, Levoine N, Paris H, N'Diaye M, Courtois A, Uriac P, Lagadic-Gossmann**  
365 **D, Fardel O, Le Ferrec E. 2012.** Induction of intracellular calcium concentration by

- 366 environmental benzo(a)pyrene involves a b2-adrenergic receptor/adenylyl cyclase/Epac-  
367 1/inositol 1,4,5-trisphosphate pathway in endothelial cells. *Journal of Biological Chemistry*  
368 **287(6):4041-4052** DOI 10.1074/jbc.M111.319970
- 369 **Nadal A, Ropero AB, Laribi O, Maillet M, Fuentes E, Soria B. 2000.** Nongenomic actions of  
370 estrogens and xenoestrogens by binding at a plasma membrane receptor unrelated to estrogen  
371 receptor alpha and estrogen receptor beta. *Proceedings of the National Academy of Sciences*  
372 **97(21):11603-11608** DOI 10.1073/pnas.97.21.11603
- 373 **Yang D, de Graaf C, Yang L, Song G, Dai A, Cai X, Feng Y, Reedtz-Runge S, Hanson**  
374 **MA, Yang H, Jiang H, Stevens RC, Wang MW. 2016.** Structural determinants of binding  
375 the seven-transmembrane domain of the glucagon-like peptide-1 receptor. *Journal of*  
376 *Biological Chemistry* **291(25):12991-13004** DOI 10.1074/jbc.M116.721977
- 377 **Zhang JH. 2008.** Quality benchmark study of polycyclic aromatic hydrocarbons in marine  
378 sediments. *Doctoral dissertation*. Dalian Maritime University.
- 379 **Zhao H, Zhao XD, Yue ZH, Zhou YB. 2014.** Effects of Benzo(a)pyrene on Antioxidant  
380 Enzyme Activity and Cytochrome P450 Gene Expression in the *P. aibuhitensis*. *Journal of*  
381 *Dalian Ocean University* **29(4):342-346** DOI 10.3969/J.ISSN.2095-1388.2014.04.004
- 382

# Figure 1

Nucleotide sequence and deduced amino acid sequence of GnRHR from *perinereis aibuhitensis*.

Initiation codon and termination codon are included in the boxes; Terminator is showed as \*;  
The approximate locations of predicted transmembrane domains 1 through 7 are noted.



## Figure 2

Multiple alignment analysis of PaGPCR with other GPCR protein.

The identical amino acid are shaded. The GenBank accession number for these proteins are as following: (A) *Platynereis dumerilii*, AKQ63061.1. (B) *Strongylocentrotus purpuratus*, XP\_003727596.1. (C) *Acanthaster planci*, XP022098630.1. (D) *Apostichopus japonicus*, PIK48567.1.

```

Perinereis_aibuhitensis -----ILLHVNIMDNITFNRTFDGSLNPNFNYIGDFVYVI 37
orphan_G-protein_coupled_receptor_56_Platynereis_dumerilii MAATTNVTGDIITQNFNLQSEHYFETLPTQSLNVNQSAAEVDASASINTDYHLIIYYVI 60
galanin_receptor_type_2-like_Strongylocentrotus_purpuratus -----MASLNGDNLTISPMPSPATVLTITANPDQGGGGGAVLELYLKIYALI 50
galanin_receptor_type_2-like_Acanthaster_planci -----MAENDLPLTHFQSI 15
putative_galanin_receptor_type_2-like_Apostichopus_japonicus -----MDPTGFVTTGSVYTEGIPPTS-----VDVLLFVLYHII 36

Perinereis_aibuhitensis GCLGLDNGFVIIVILHSRKRMRNKLGNLFLNQSVVDLVAIVFLLCNSPSVP-----TL 91
orphan_G-protein_coupled_receptor_56_Platynereis_dumerilii GACGIFGNILVCKVMFSSATLARKITNWFHINQSLVDFAVSFFLTQADVQ-----GE 113
galanin_receptor_type_2-like_Strongylocentrotus_purpuratus GLLGVNGNGIVCLVFTIKRRQFSITNYLILNQSVIDLDSIFFILIHYPNGPISETA 110
galanin_receptor_type_2-like_Acanthaster_planci GITGICGNALVGVVIKIR-FMHTLTNAPFNQALIDLFGSFMILLNLLVP-----IPD 68
putative_galanin_receptor_type_2-like_Apostichopus_japonicus GFLGIFGNGVVIIVFLANRKFVRSHTNLLHNLQAIMDFVVAIIFLLDRFGP-----SLYK 91

Perinereis_aibuhitensis GSASNISLEFYCRHWDSNYLFAAVTWSTVNLVAITLERYLEVVEHLRYSFFTRRRKRV 151
orphan_G-protein_coupled_receptor_56_Platynereis_dumerilii PPHSGIAGELYCRHWATKLFNLGFLVSTVNLVALTHERYLAUVHPIWHKTSFSKTKATV 173
galanin_receptor_type_2-like_Strongylocentrotus_purpuratus NIPSRGLAEFFCRHWDSYPLWALYIASTANLVLSLERYFATCRPVIIHRNFFTIVRRKRW 170
galanin_receptor_type_2-like_Acanthaster_planci PLPSNSNGVLLCRHWLSGYFNWALFVSTVNLVALTHERYLAIVFPRYQVLGTRKNALI 128
putative_galanin_receptor_type_2-like_Apostichopus_japonicus LITNETLSEMLCRHWDSYELLWAFYIASTQNLVMSLERYFATCRPVKHRNYFTIRGAKI 151

Perinereis_aibuhitensis IVAVVWLVGFIPIVTSVITSPAG-----ADGTCQKHRAWSSRLMAALVGFYALFFGELL 206
orphan_G-protein_coupled_receptor_56_Platynereis_dumerilii LIALVWLVGFPVWNASYSIVTSSNED-----GVCAIYAIWPSITVRRFPGLVTLVLLQVLI 227
galanin_receptor_type_2-like_Strongylocentrotus_purpuratus AMLCVWVYGAIVYQYLPVDTFSA-----DWR-CHPNWPNRVVQRFGVLLFSLEYLI 222
galanin_receptor_type_2-like_Acanthaster_planci IIVIVWVSAFLFTSYGVFIIRYKYG-----GQC-----KQKLVHAEVLEGLVAVFAVTELL 177
putative_galanin_receptor_type_2-like_Apostichopus_japonicus GIAGIWLFGLVYQSYWIFVFFFEF-----SSQSCFPLWNTRTLQACMGVFFVFLMEVLI 204

Perinereis_aibuhitensis PVVIMIVCYTQMIMTFNLKVRPSDPS-----IMISESEKRRSERMLRVRKSLIKITML 258
orphan_G-protein_coupled_receptor_56_Platynereis_dumerilii PPTFIIIPAYGSIALKLYRKLKSD-----GAARKGDETIQRGMNRTVTKTLV 272
galanin_receptor_type_2-like_Strongylocentrotus_purpuratus PLIIMTCSYVSIILMLRNRTK-----SHGKVQVNAFQRAKRNVTITLTC 265
galanin_receptor_type_2-like_Acanthaster_planci PVIVMLVVVAHITVVLKRGAGRIQPGPAA---AVPSTGTAPEGQGESLMRARNRTFKTLL 234
putative_galanin_receptor_type_2-like_Apostichopus_japonicus PPIVMTFSYVNIILMLKRR-----GQKSGS-VFQRAKRNVTITLTC 244

Perinereis_aibuhitensis PVVIMIVCYTQMIMTFNLKVRPSDPS-----IMISESEKRRSERMLRVRKSLIKITML 258
orphan_G-protein_coupled_receptor_56_Platynereis_dumerilii PPTFIIIFANGSIALKLYRKLKSD-----GAARKGDETIQRGMNRTVTKTLV 272
galanin_receptor_type_2-like_Strongylocentrotus_purpuratus PLIIMTCSYVSIILMLRNRTK-----SHGKVQVNAFQRAKRNVTITLTC 265
galanin_receptor_type_2-like_Acanthaster_planci PVIVMLVVVAHITVVLKRGAGRIQPGPAA---AVPSTGTAPEGQGESLMRARNRTFKTLL 234
putative_galanin_receptor_type_2-like_Apostichopus_japonicus PPIVMTFSYVNIILMLKRR-----GQKSGS-VFQRAKRNVTITLTC 244

Perinereis_aibuhitensis MVSIVFVICWIGDQVYFLFN--IRVIKDLQQLTTIVVSLAFLNCCINBFYITCQYNDF 316
orphan_G-protein_coupled_receptor_56_Platynereis_dumerilii LVAICFVACWSWNQIYLLMMN--LGFREDYSSNFYHFTVIAVFINSCVNPFIYALKYDFF 330
galanin_receptor_type_2-like_Strongylocentrotus_purpuratus IVFVSVVVCWTPTELSYLAYN--LGHDFNFESAVHDVLKGLVACNLGVNPFYIYAFKYEHF 323
galanin_receptor_type_2-like_Acanthaster_planci LVFVAETICWTPNEVFLLFN--LGVVNLSTIFFVIVAMVSTNSCLNPFYIYAIKPKQF 292
putative_galanin_receptor_type_2-like_Apostichopus_japonicus LVFVSVVICWTPTEFGIILYN--CGRPYDFEGTFHYVATVVLVLCNCTAFYIYTFKWEQF 302

Perinereis_aibuhitensis QEATRRLLKIKKESENSERSTLDLSNQV----- 345
orphan_G-protein_coupled_receptor_56_Platynereis_dumerilii KKAAYQLFCTKMLGIRPNAIEDQS----- 354
galanin_receptor_type_2-like_Strongylocentrotus_purpuratus QSELKKIFCSMCAAGNRISTESRGTVLSPANNSNNTP----- 361
galanin_receptor_type_2-like_Acanthaster_planci RKALKTLFG--RQGGIEDESTLATVATAHD----- 320
putative_galanin_receptor_type_2-like_Apostichopus_japonicus QNYLKRMFGRCLGVNRIIDVNTVSAVAEPDQDTLNRSSDTGKQAATA----- 350

```

## Figure 3

Analysis of transmembrane region of PaGPCR

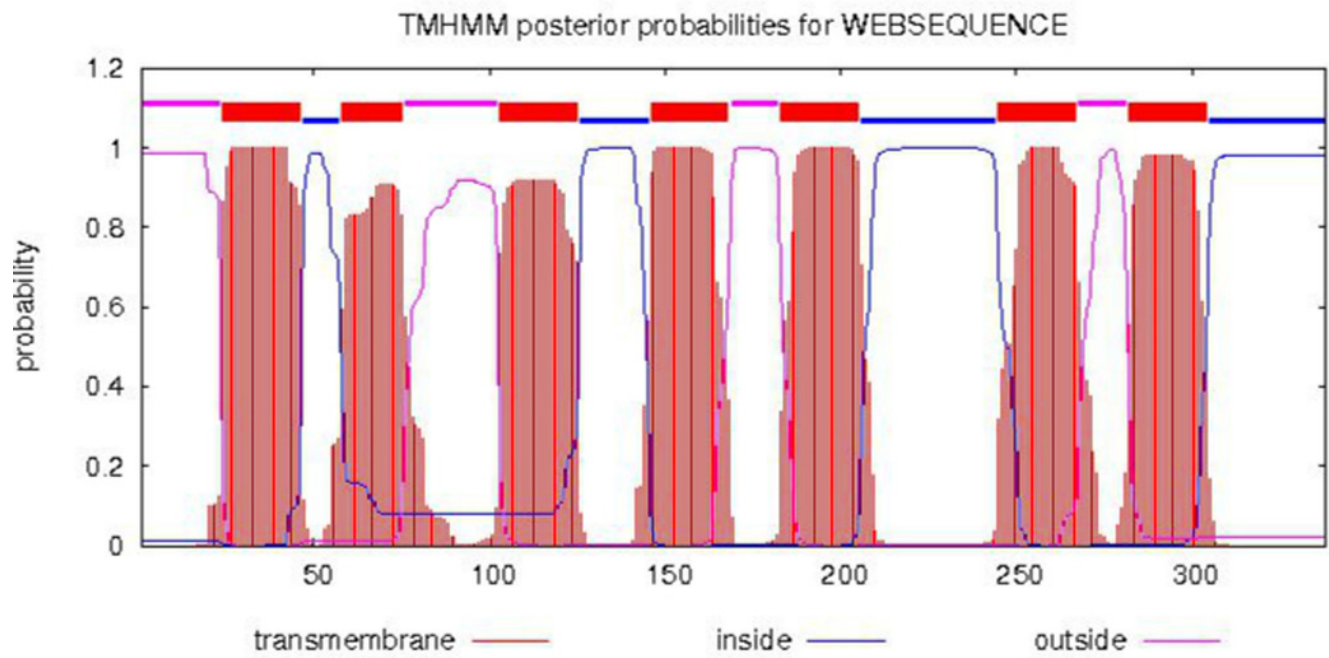


## Figure 4

The three dimensional structure of PaGPCR

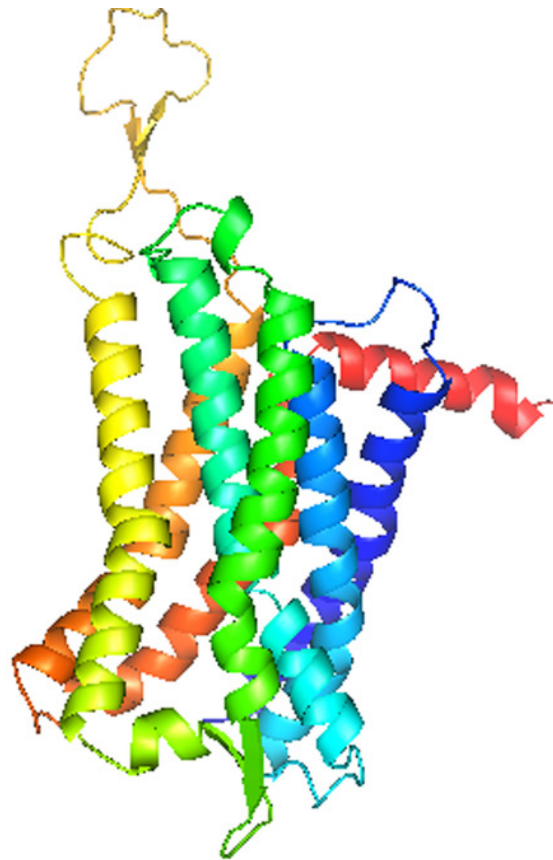


## Figure 5

the full cDNA sequence and deduced amino acid sequence of PaPKA.

Red fonts show initiation codon and termination codon; Terminator is showed as\*; The red bars under the sequences indicated the ATP active site, Ser /Thr active site and PKA regulatory subunit binding site was underlined with red line, conservative phosphorylation site is boxed in green.

```

1  GTCGAAGAGATCGAGGTGGAATATTCAGACATAATTTTTGAGAAGCTGGTTCGAGAGTTCCTGATTTCTGGCCGGTTAATTCCTCTGGATCACCACGGACTAG
106 GTAGTTTACCACACGGTAGCCATCGSAAATGCTGCAACAGCAAAGAAAGGCGATCCAGAGAATGTCAAAGAGTTCCTAGCCAAAGCTAAAGAGGACTTCAACAAG
1  M G N A A T A K K G D P E N V K E F L A K A K E D F N K
211 AAATGGGAAGAGCCATCATGTAACACTGCATCACTAGATGACTTCGACAGAATTAACCCCTGGGAACAGGGTCATTTGGACGGGTCATGCTGGTTCAGCACAAA
29  K W E E P S C N T A S L D D F D R I K T L G T G S F G R V M L V Q H K
316 GCCACGAAGGAGTACTATGCCATGAAGATTTTAGATAAAACAAAAGGTAGTGAAGCAAGTTGAACACACATTGAATGAAAAGAAAATTCGTCCGCCATA
64  A T K E Y Y A M K I L D K Q K V V K L K Q V E H T L N E K K I L S A I
421 TCATTTCATTCTTAGTGAGCCTAGAGTACAGTTTTAAGGATAACTCAAATTTGTACATGGTATTGGAGTTCGTGACAGGAGGTGAAATGTCTCACATCTGCGA
99  S F P F L V S L E Y S F K D N S N L Y M V L E F V T G G E M F S H L R
526 AGAATTGGCCGATTTAGTGAAACTCACAGCCGATTTTATGCTGCACAAGTATGCATGGTATTTGAATATCTGCACAATCTAGACACACTGTACAGAGATTGAAG
134 R I G R F S E T H S R F Y A A Q V C M V F E Y L H N L D T L Y R D L K
631 CCAGAAAATATCTGATTGATGACACTGGTCACTTGAGAGTAACAGACTTCGGTTTTGCCAACCGCTAAAAGGCAGGACATGGACGTTGTGTGGCACACCAGAG
169 P E N I L I D D T G H L R V T D F G F A K R V K G R T W T L C G T P E
736 TACCTGGCCCCAGAAATCATCTTGAGCAAGGGCTACAACAAAGCCGTAGACTGGTGGGCGCTTGGAGTCCCTGTTTATGAAATGGCAGCTGGATACCCACCTTTC
204 Y L A P E I I L S K G Y N K A V D W W A L G V L V Y E M A A G Y P P F
841 TTTGCTGACCAGCCAATCCAAATCTATGAGAAGATTGTCTCAGGAAAGGTGCGCTTCCCATCTCACTTTAGTTCTGATTGAAGGATCTTTGAAGAATCTGCTA
239 F A D Q P I Q I Y E K I V S G K V R F P S H F S S D L K D L L K N L L
946 CAGGTAGACTTGACAAAACGTTATGGAACCTGAAGAATGGGGTCAACGATATCAAGAATCACAAGTGGTTCCTCCACCACAGACTGGATTGCTATCTACCAGAAA
274 Q V D L T K R Y G N L K N G V N D I K N H K W F S T T D W I A I Y Q K
1051 AAGTTGAAGCACCCCTTCATTCCTCAAGTGCAAAGGCCAGGTGACTACAGCAACTTTGATGACTATGAGGAAGAACCCTGAGAATTTTCGTCAACGGAAAAATGT
309 K V E A P F I P K C K G P G D Y S N F D D Y E E E P L R I S S T E K C
1156 GCCAAGGAGTTTGCAGACTTCTGAGACAGTTGGCTTGTAGGTGGCTAGTGTGTGTGGGGAACTAAAGACTGTGATGACCATTCTGTGTTTCATGGTCTATCACT
344 A K E F A D F *
1261 GGCAGCTGGCTGAAGATCTGCGGCCACATACCACACAATCTCTCAAAGAATACATCCTTTGTGCATTAACAAATGTATATATACTTAATCATATCACATTGCGT
1366 AATTGTAACAAGGTGAATTCAGTTTCATATGTGTCAATGAGGTAAGAGAGAGGGCTTCGATCCCAGGTGTGGCATGTCCCTGAGGCTGCGCTATTGGTCCGAGGT
1471 AAGCCAGGTGCTTCAGCTCGCACCCAGGCTGCCTCAAAGCTACCTTGGTCGTCTACTCGCCGAAGTACTGATTTACCTTGTGTGTGGCCTCCAGATTTGT
1576 GTGGGGCAGACTGGTGGAGGATTAGGCTTTAATTGCTTTGCTGAAGTGCACACCGGTCCAGAAGCCAGGCTATCTTCAAATACACAGTTAATACCATATAT
1681 TAACCTATCATTACAACCTTACTGACCACTTGTTTCACATTTAGGTCATTTGCTGCACCTTTTATGTATACAGGTGGTCCATCTGAAACAATCTCTGAACATTTG
1786 AATTATATCCATTGTAAGGAAGTGCAAACTTCTCTGTGCTGTGCTCCTCCACTCCCGTGTGCTTCTTTCTCTGCTGTGAACTTTGAATCAGAGAGAAACAA
1891 CACTTTATTTGTATGATGTCAAATATTGTACTTTGGTAAGGCCACCTCCTAAGTGGTGGTTCATCAAGACTTGTATATAGTTTGTGAGCAGTTGGCTTTTGGGT
1996 AGAGTAGGAGTTTCTGTTTCATCATACTAGGTGGGATGACACCATCTCCCGCATACCAGTAGTACTGTGTAGTAGCAATAGCCCGCCATAAGGCCATGAGTCTCC
2101 ATTGTTTCAGCTAATGTAGCTAGGCTCAAGTCATAAGTCATGATAACATATAATGGCATTATTTGTAGTACTGATGATGAGAGAATATTATCTTTGTCAAGACA
2206 AACTTATTTTACTTTTATATAACTGACTTGTATGTACAGACGTCGAAGGCTGTATGAAGTGAAGAATTTGTTGCTTGTATGTGTAGTGTATAAAATGTGTATATCT
2311 ATCTCTGCATATTTTGTGTTTGTATGTCAATCCACAATGCTTCAAATTTATCTTGAACCATGTACTTGACTAATCTAATTTGTGATTTGAAAAGGTAATTGGA
2416 GTTGTGCTGAATTAGATAGGTATGCTTCTGACATTTGTGTAACACTACTACAGTGAGTCCCATTTGTGATGGGTCCTACTCATGAATGTTGTTATATTTGTATA
2521 TACTAAAAATAATTTATGCTGGTTCATGAAGATGTACAAAAAATATTTTTCAAATGGCTAAGGATGGTTTTGTAGAAATTTGTACTAAGGGTCAGCAGTTAA
2626 CAAACCCCATGAAAAAAAAAAAAAAAAAAAAAAAAAAAAA

```

## Figure 6

Multiple alignment of PaPKA with other PKA.

The identical amino acid are shaded. The GenBank accession number for these proteins are as following: (A) *Aplysia californica*, NP\_001191420.1. (B) *Xenopus tropicalis*, NP\_001164667.1. (C) *Branchiostoma floridae*, XP\_002600447.1. (D) *Danio rerio*, NP\_001030148.1. (E) *Octopus bimaculoides*, XP\_014777153.1. (F) *Lingula anatina*, XP\_013409439.1. (G) *Crassostrea gigas*, XP\_011439335.1. (H) *Biomphalaria glabrata*, XP\_013072294.1. (I) *Salmo salar*, XP\_014071121.1. (J) *Gallus gallus*, XP\_015146370.1.

Perinereis_aibuhitensis	MGNAATAK-----KGDPEEN---VKBFLAKAKBDFNKWBEPSCNTASLDDFDRIKTLGTGSFGRVMIQVHK-ATKEYYA	70
Aplysia_californica	MGNAATAK-----KGDPAEN---VKBFLAKAKBDFNKWBEPSCNTASLDDFDRIKTLGTGSFGRVMIQVHKGERRNFYA	72
Xenopus_tropicalis	MGNAATAK-----KGNIEIES---VKBFLAKAKBDFNKWBEPSCNTASLDDFDRIKTLGTGSFGRVMIQVHKH-GAEQYYA	71
Branchiostoma_floridae	MAAKATPKGSGHGKATAIGKISKHGDGGSYSDSVKBFLAKAKBDFNKWBEPSQNTAALDFDRIKTLGTGSFGRVMIQVHK-ATQNEYA	89
Danio_erio	MGNAATAK-----KGNELSES---VKBFLAKAKBDFNKWBEPSQNTAALDFDRIKTLGTGSFGRVMIQVHKH-ASDQYYA	71
Octopus_bimaculoides	MGNAATAK-----KGDPAEN---VKBFLAKAKBDFNKWBEPSQNTAALDFDRIKTLGTGSFGRVMIQVHK-ANKEYYA	71
Lingula_anatina	MGNAATAK-----KLDPAEN---VKBFLAKAKBDFNKWBEPSQNTAALDFDRIKTLGTGSFGRVMIQVHK-QSKQYYA	71
Crassostrea_gigas	MGNAATAK-----KGDPAEN---VKBFLAKAKBDFNKWBEPSQNTAALDFDRIKTLGTGSFGRVMIQVHK-ANKDEYA	71
Biomphalaria_glabrata	MGNAATAK-----KGDPAEN---VKBFLAKAKBDFNKWBEPSQNTAALDFDRIKTLGTGSFGRVMIQVHKGENKSFYA	72
Salmo_salar	MGNAATAK-----KGNESQES---VKBFLAKAKBDFNKWBEPSQNTAALDFDRIKTLGTGSFGRVMIQVHKH-GTEQYYA	71
Gallus_gallus	MGNAATAK-----KGNIEISET-VKBFLAKAKBDFNKWBEPSQNTAALDFDRIKTLGTGSFGRVMIQVHKH-ATEQYYA	74

Perinereis_aibuhitensis	MKILDKQKVVVKLQVEHTLNEKKILSAISFPFLVSRLEYSEKDNSNLYMVEFVTTGGEMFSLRRIIGRFSEPHSRFYAAQIVLVLFEYLHSL	160
Aplysia_californica	MKILDKQKVVVKLQVEHTLNEKKILQSIINFPFLVSRLEYSEKDNSNLYMVEFVTTGGEMFSLRRIIGRFSEPHSRFYAAQIVLVLFEYLHSL	162
Xenopus_tropicalis	MKILDKQKVVVKLQVEHTLNEKKILQAVNFPFLVSRLEYSEKDNSNLYMVEFVTTGGEMFSLRRIIGRFSEPHSRFYAAQIVLVLFEYLHSL	161
Branchiostoma_floridae	MKILDKQKVVVKLQVEHTLNEKKILQAVSFPFLVSRLEYSEKDNSNLYMVEFVTTGGEMFSLRRIIGRFSEPHSRFYAAQIVLVLFEYLHSL	179
Danio_erio	MKILDKQKVVVKLQVEHTLNEKKILQAVSFPFLVSRLEYSEKDNSNLYMVEFVTTGGEMFSLRRIIGRFSEPHSRFYAAQIVLVLFEYLHSL	161
Octopus_bimaculoides	MKILDKQKVVVKLQVEHTLNEKKILQAVSFPFLVSRLEYSEKDNSNLYMVEFVTTGGEMFSLRRIIGRFSEPHSRFYAAQIVLVLFEYLHSL	161
Lingula_anatina	MKILDKQKVVVKLQVEHTLNEKKILQAVSFPFLVSRLEYSEKDNSNLYMVEFVTTGGEMFSLRRIIGRFSEPHSRFYAAQIVLVLFEYLHSL	161
Crassostrea_gigas	MKILDKQKVVVKLQVEHTLNEKKILQAVSFPFLVSRLEYSEKDNSNLYMVEFVTTGGEMFSLRRIIGRFSEPHSRFYAAQIVLVLFEYLHSL	161
Biomphalaria_glabrata	MKILDKQKVVVKLQVEHTLNEKKILQAVSFPFLVSRLEYSEKDNSNLYMVEFVTTGGEMFSLRRIIGRFSEPHSRFYAAQIVLVLFEYLHSL	162
Salmo_salar	MKILDKQKVVVKLQVEHTLNEKKILQAVSFPFLVSRLEYSEKDNSNLYMVEFVTTGGEMFSLRRIIGRFSEPHSRFYAAQIVLVLFEYLHSL	161
Gallus_gallus	MKILDKQKVVVKLQVEHTLNEKKILQAVNFPFLVSRLEYSEKDNSNLYMVEFVTTGGEMFSLRRIIGRFSEPHSRFYAAQIVLVLFEYLHSL	164

Perinereis_aibuhitensis	DLIYRDLKPENLLIDDTGHLRVTDFGFAKRVKGRWTWLCGTPEYLAPEIILSKGYNKAVDWWALGVLVYEMAAGYPPFFADQPIQIYEKI	250
Aplysia_californica	DIMYRDLKPENLLIDSYGYLKVTDDFGFAKRVKGRWTWLCGTPEYLAPEIILSKGYNKAVDWWALGVLVYEMAAGYPPFFADQPIQIYEKI	252
Xenopus_tropicalis	DLIYRDLKPENLLIDQQGYIQVTDDFGFAKRVKGRWTWLCGTPEYLAPEIILSKGYNKAVDWWALGVLVYEMAAGYPPFFADQPIQIYEKI	251
Branchiostoma_floridae	DIIYRDLKPENLLIDQLGYLKVTDDFGFAKRVKGRWTWLCGTPEYLAPEIILSKGYNKAVDWWALGVLVYEMAAGYPPFFADQPIQIYEKI	269
Danio_erio	DLIYRDLKPENLLIDQHGYYIQVTDDFGFAKRVKGRWTWLCGTPEYLAPEIILSKGYNKAVDWWALGVLVYEMAAGYPPFFADQPIQIYEKI	251
Octopus_bimaculoides	DIIYRDLKPENLLIDSSGYLKVTDDFGFAKRVKGRWTWLCGTPEYLAPEIILSKGYNKAVDWWALGVLVYEMAAGYPPFFADQPIQIYEKI	251
Lingula_anatina	DIMYRDLKPENLLIDSTGYLKVTDDFGFAKRVKGRWTWLCGTPEYLAPEIILSKGYNKAVDWWALGVLVYEMAAGYPPFFADQPIQIYEKI	251
Crassostrea_gigas	DIMYRDLKPENLLIDTMSGYLKVTDDFGFAKRVKGRWTWLCGTPEYLAPEIILSKGYNKAVDWWALGVLVYEMAAGYPPFFADQPIQIYEKI	251
Biomphalaria_glabrata	DLVYRDLKPENLLIDPQGYCKVTDDFGFAKRVKGRWTWLCGTPEYLAPEIILSKGYNKAVDWWALGVLVYEMAAGYPPFFADQPIQIYEKI	252
Salmo_salar	DLIYRDLKPENLLIDHQGYIQVTDDFGFAKRVKGRWTWLCGTPEYLAPEIILSKGYNKAVDWWALGVLVYEMAAGYPPFFADQPIQIYEKI	251
Gallus_gallus	DLIYRDLKPENLLIDQQGYIQVTDDFGFAKRVKGRWTWLCGTPEYLAPEIILSKGYNKAVDWWALGVLVYEMAAGYPPFFADQPIQIYEKI	254

Perinereis_aibuhitensis	VSGKVRFPSPHFSSDLKDLLRNLLQVDLTKRYGNLKNGVNDIKHKKWFATDWTIAIYQKRVKVEAPFIPKCRGGDTSNFDDYEBEEDVRISST	340
Aplysia_californica	VSGKVRFPSPHFSSDLKDLLRNLLQVDLTKRYGNLKNGVNDIKHKKWFATDWTIAIYQKRVKVEAPFIPKCRGGDTSNFDDYEBEEDVRISST	342
Xenopus_tropicalis	VSGKVRFPSPHFSSDLKDLLRNLLQVDLTKRYGNLKNGVNDIKHKKWFATDWTIAIYQKRVKVEAPFIPKCRGGDTSNFDDYEBEEDVRISST	341
Branchiostoma_floridae	VSGKVRFPSPHFSSDLKDLLRNLLQVDLTKRYGNLKNVNDIKHKKWFATDWTIAIYQKRVKVEAPFIPKCRGGDTSNFDDYEBEEDVRISAT	359
Danio_erio	VSGKVRFPSPHFSSDLKDLLRNLLQVDLTKRYGNLKNGVNDIKHKKWFATDWTIAIYQKRVKVEAPFIPKCRGGDTSNFDDYEBEEDVRISVT	341
Octopus_bimaculoides	VSGKVRFPSPHFSSDLKDLLRNLLQVDLTKRYGNLKNGVNDIKHKKWFATDWTIAIYQKRVKVEAPFIPKCRGGDTSNFDDYEBEEDVRISST	341
Lingula_anatina	VSGKVRFPSPHFSSDLKDLLRNLLQVDLTKRYGNLKNGVNDIKHKKWFATDWTIAIYQKRVKVEAPFIPKCRGGDTSNFDDYEBEEDVRISST	341
Crassostrea_gigas	VSGKVRFPSPHFSSDLKDLLRNLLQVDLTKRYGNLKNGVNDIKHKKWFATDWTIAIYQKRVKVEAPFIPKCRGGDTSNFDDYEBEEDVRISST	341
Biomphalaria_glabrata	VSGKVRFPSPHFSSDLKDLLRNLLQVDLTKRYGNLKNGVNDIKHKKWFATDWTIAIYQKRVKVEAPFIPKCRGGDTSNFDDYEBEEDVRISST	342
Salmo_salar	VSGKVRFPSPHFSSDLKDLLRNLLQVDLTKRYGNLKNGVNDIKHKKWFATDWTIAIYQKRVKVEAPFIPKCRGGDTSNFDDYEBEEDVRISST	341
Gallus_gallus	VSGKVRFPSPHFSSDLKDLLRNLLQVDLTKRYGNLKNGVNDIKHKKWFATDWTIAIYQKRVKVEAPFIPKCRGGDTSNFDDYEBEEDVRISST	344

Perinereis_aibuhitensis	EKCAKEFAADF	350
Aplysia_californica	EKCAKEFAADF	352
Xenopus_tropicalis	EKCAKEFAADF	351
Branchiostoma_floridae	EKCAKEFAADF	369
Danio_erio	EKCAKEFAADF	351
Octopus_bimaculoides	EKCAKEFAADF	351
Lingula_anatina	EKCAKEFAADF	351
Crassostrea_gigas	EKCAKEFAADF	351
Biomphalaria_glabrata	EKCAKEFAADF	352
Salmo_salar	EKCAKEFAADF	351
Gallus_gallus	EKCAKEFAADF	354

## Figure 7

The three dimensional structure of PKA from *P. aibuhitensis*



## Figure 8

Molecular phylogenetic analysis of PaGPCR related to GPCR of other invertebrates and vertebrates

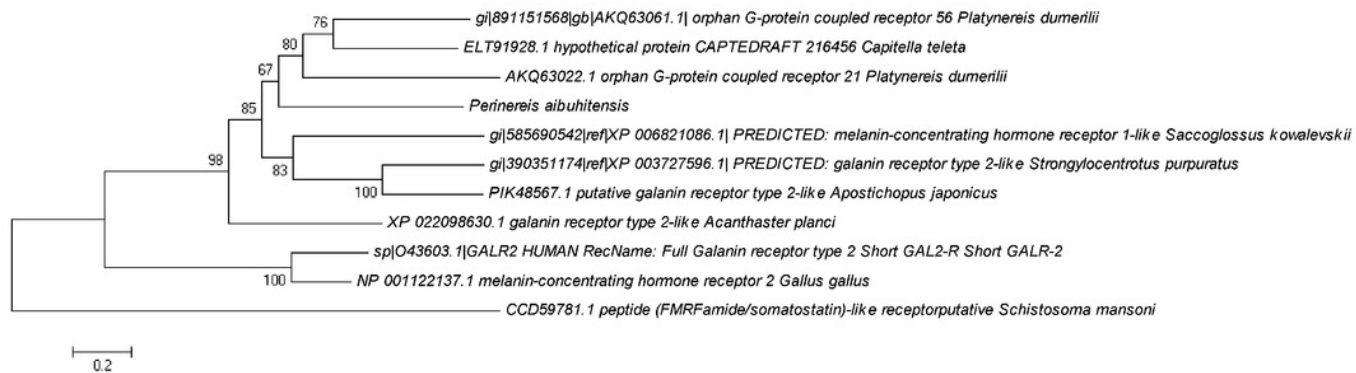


## Figure 9

Molecular phylogenetic analysis of PaPKA related to PKA of other invertebrates and vertebrates

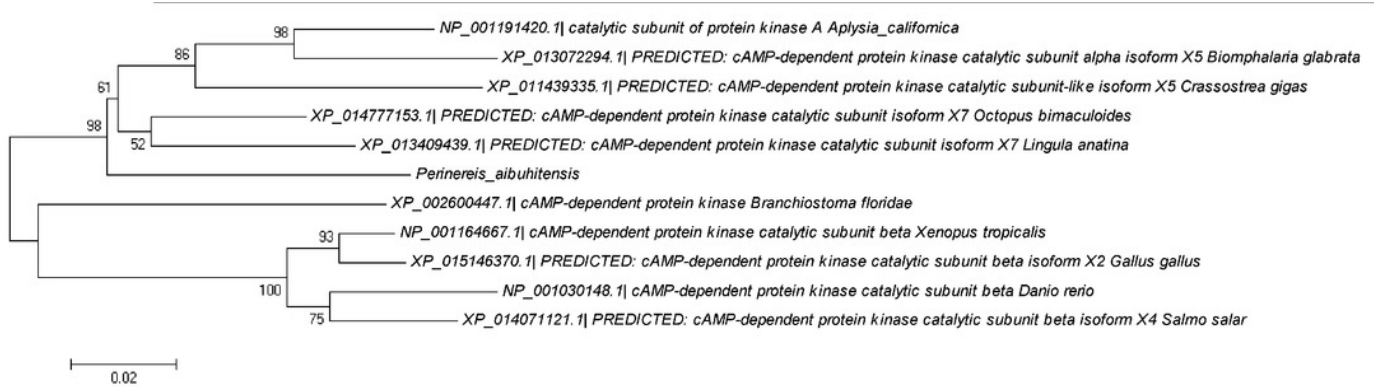


## Figure 10

The relative expression level of PaGPCR and PaPKA cDNAs under various B(a)p concentration exposure. A PaGPCR, B PaPKA. Different lowercase letters indicate significant difference ( $P < 0.05$ ). all data as mean+SD. N= four worms.

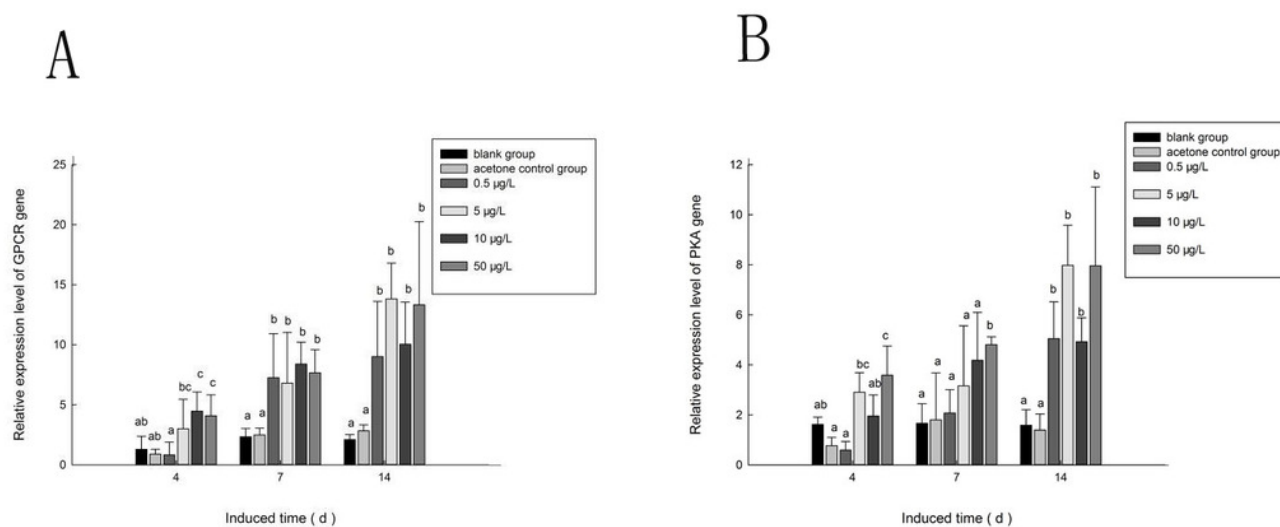


**Table 1** (on next page)

The primers used in this study

Primer name		sequence (5'-3')
RACE	GPCR - F1	TGAGAAACGTCGAAGCGAAAGG
	GPCR - R1	ATATTCGACGCTGACCCTAAGG
	PKA-F1	GATACCCACCTTTCTTTGCTGACC
	PKA-F2	GGTGCGCTTCCCATCTCACTTT
	PKA-R1	CAATAGCGCAGCCTCAGGGACA
	UPM Long	CTAATACGACTCACTATAGGGCAAGCAG TGGTATCAACGCAGAGT
	UPM Short	CTAATACGACTCACTATAGGGC
Real time PCR	$\beta$ -actin-R	CGAAGTCCAGAGCAACATAG
	$\beta$ -actin-F	GGGCTACTCCTTCACCACCA
	GPCR-R3	CCGTAAAAGCCTCATCAAGACA
	GPCR-F3	TTGGCAGGTGTAAATGAATGG
	PKA-F3	GACCAGCCAATCCAAATCTATG
	PKA-R3	GACCCCATTCCTTCAGGTTTCC

1

2

3

4